INHERENT DAMPING DURING NONLINEAR SEISMIC RESPONSE

Dionisio Bernal

Civil and Environmental Engineering Department, Center for Digital Signal Processing, Northeastern University, Boston MA 02115

Abstract

An approach to interrogate measured response on the behavior of inherent damping during nonlinear excursions is presented. The scheme computes a signal that approximates the base shear (to within a scalar) and decides on the inherent damping during nonlinear excursions on the premise that the derivative of this signal, with respect to time, is small within these segments. Preliminary results suggest that the inherent damping model should include a reduction in effectiveness when hysteretic dissipation is activated.

Introduction

A long-standing open question in evaluating the response of buildings to strong earthquakes is whether the model used to capture energy dissipation not associated with damage should be modified, or remain unchanged, when hysteretic behavior is activated [1-6]. This question has been difficult to resolve because the inherent damping model is a surrogate for the aggregate of a number of unspecified mechanisms, calibrated to match decay rates observed for small vibrations, but for which there is no mechanistic support. We note in passing that use of mass and stiffness matrices to specify the classical damping model (wherein damped and undamped eigenvectors coincide, as is the case in the Rayleigh model or in the more general Caughey series [7,8]) is justified by the simplicity that it brings but is not mechanistically supported.

Lack of a mechanistic model for inherent damping indicates that (apart from consistency from an energy perspective) the only way to decide on the merit of any postulated model is from seismic response observations. On the question of coupling between hysteresis and pseudo-viscosity the main obstacle to a data-supported resolution comes from the fact that the stiffness restoring forces cannot be directly measured and cannot be estimated with sufficient accuracy from a model to allow computation of the damping forces from equilibrium. We attempt to make some headway by shifting the focus from dynamic equilibrium to the rate of change of the terms in the equilibrium equations and by simplifying the spatial distribution of the damping forces (to be described). The information infused to arrive at a workable scheme is the contention that the rate of change of a scalar measure of the unknown stiffness contribution, not always, but in many cases, is small enough to be discarded. We designate the interrogation scheme that results from the previous ideas as the “Inherent Damping Nonlinear Behavior” (IDNB) extractor. This paper

presents the theoretical support of IDNB, reports on the current progress in its validation and limitations and includes some initial results from application to data recorded during strong shaking in buildings from the CSMIP database.

The Basic Ideas

Let $I(t), D(t), R(t)$represent the vectors of inertia, damping and restoring forces during a generally nonlinear response. Equilibrium for base excitation requires that

$$I(t) + D(t) + R(t) = 0 \tag{1}$$

our goal is to determine if something can be said, primarily from data, about what happens to the mechanism that generates $D(t)$during intervals when $R(t)$reflects significant nonlinearity. To move forward we pre-multiply by the transpose of the column vector of ones ($r$when used subsequently) and introducing obvious notation write

$$V_R(t) = -\big(V_I(t) + V_D(t)\big) \tag{2}$$

To make things tractable we take the damping forces at any time as those that would have existed if the damping matrix was invariant, times a modulation that is to be determined, namely, we take them as

$$D(t) = \rho(t) C_0 \dot{u}(t) \tag{3}$$

where $\dot{u}(t)$ =vector or relative velocities and $\rho(t)$is a scalar. Differentiating Eq.3 with respect to time and substituting the result into the derivative of Eq.2 writes

$$\dot{V}_R(t) = -\Big(\dot{V}_I(t) + \rho(t) r^T C_0 \ddot{u}(t) + \dot{\rho}(t) r^T C_0 \dot{u}(t)\Big) \tag{4}$$

Results of numerical simulations suggest that the third term on the right-hand side of Eq.4 is small compared to the other two, so we simplify by taking $\dot{\rho}(t) = 0$ and get

$$\dot{V}_R(t) = -\Big(\dot{V}_I(t) + \rho(t) r^T C_0 \ddot{u}(t)\Big) \tag{5}$$

Assume, temporarily, that the disjointed time intervals when inelasticity is extensive have been determined and have been aggregated into the time segment $\tilde{t}$. Restricting evaluation of Eq.5 to these times one has

$$\dot{V}_R(\tilde{t}) = -\Big(\dot{V}_I(\tilde{t}) + \rho(\tilde{t}) r^T C_0 \ddot{u}(\tilde{t})\Big) \tag{6}$$

At this point we replace $\rho(\tilde{t})$ with a constant $\bar{\rho}$ and while the equality cannot hold at all times after this replacement, it can be preserved at the level of norms, so we take the 2-norm and get

$$\left\|\dot{V}_R(\tilde{t})\right\| = \left\|\left(\dot{V}_I(\tilde{t}) + \bar{\rho} r^T C_0 \ddot{u}(\tilde{t})\right)\right\| \tag{7}$$

where it's a simple matter to show that

$$\dot{V}_R(\tilde{t}) = r^T K_T(\tilde{t}) \dot{u}(\tilde{t}) \tag{8}$$

with K_T=structure's tangent stiffness. Substituting Eq.8 into Eq.7 writes

$$r^T K_T(\tilde{t}) \dot{u}(\tilde{t}) = -\left(\dot{V}_I(\tilde{t}) + \rho(\tilde{t}) r^T C_0 \ddot{u}(\tilde{t})\right) \tag{9}$$

Since $K_T(\tilde{t})$ is not known the *lhs* of Eq.9 cannot be explicitly evaluated, but if the term is small, relative to$\|r^T C_0 \ddot{u}(\tilde{t})\|$, it appears reasonable to decide on $\bar{\rho}$as the value that minimizes the *rhs* of the Eq.7. We can summarize as follows:

- The IDNB scheme computes a value, $\bar{\rho}$, such that the inherent damping during nonlinear excursions is estimated as $\xi_{non} = \bar{\rho}\xi$, where $\xi$is the damping ratio that holds if the structure behaved linearly. The value of $\bar{\rho}$is taken as that which minimizes the rhs of Eq.7

Is the Discarded Term Small Enough?

A necessary condition for minimization of the *rhs* Eq.7 to give meaningful results for $\bar{\rho}$is that

$$\|r^T K_T(\tilde{t}) \dot{u}(\tilde{t})\| \ll \left\|\left(r^T C_0 \ddot{u}(\tilde{t})\right)\right\| \tag{10}$$

In a shear building where first story yielding dominates the *lhs* of Eq.10 is exactly zero (in the absence of strain hardening) and the inequality is guaranteed satisfied. In general, however, one does not know if this is so, and it seems that all that can be said is that if it's not satisfied $\bar{\rho}$will be overestimated. It is not unreasonable to wonder whether the constraint in Eq.10 is ever satisfied when real data is considered so we tried to see if a relation that shed some light on the question could be derived. A useful expression obtained using approximations with bounded errors could not be found but a very rough result is as follows: assume the damping matrix C_0 is stiffness proportional with a fundamental mode damping ξ, so that $C_0 = 2\xi\omega^{-1}K$and express the tangent stiffness as a fraction of the initial matrix, namely $K_T = \eta K$. With these replacements and taking $b = r^T K$one finds that Eq.10 translates to $\eta\|b\dot{u}(\tilde{t})\| \ll 2\xi\omega^{-1}\|b\ddot{u}(\tilde{t})\|$ which, taking $\|b\ddot{u}(\tilde{t})\| \cong \omega\|b\dot{u}(\tilde{t})\|$gives $\eta \ll 2\xi$. The foregoing states that satisfaction of the constraint hinges on the tangent stiffness scaling being small compared to twice the critical damping ratio of the fundamental mode. This examination is too rough to allow

solid assertions, but it appears to leave open the possibility that the constraint may be satisfied, which would not be the case if the result had been $\eta \ll 0.02\xi$.

On the selection of $\tilde{t}$

The signal in Eq.9 is a reordered version of the signal of Eq.5, subsequently truncated to a length $\tilde{t}$. The reordering is done with the goal of making the early values have a high probability of being points when inelasticity is extensive, with the approach used thus far being to order the points in increasing absolute value. The truncating length $\tilde{t}$is in principle the aggregate length of all the yielding segments (although a fraction should also work) and in the numerical section we've taken it to be within 1 to 2% of the strong motion.

Inherent Damping Models

Since the inherent damping behavior is unknown, validation of IDNB must be carried out in simulations. Specifically, one postulates various inherent damping models that are coupled with the hysteresis response as well as constant damping one and the goal is to determine whether or not IDNB can discriminate between them using signals from a limited number of floors (plus information on the location of the sensors and the relative values of the story weights). For this purpose, we selected 3 previously proposed inherent damping models plus a new one introduced here designated as the $CSMIP\kappa$ model. Nonlinear damping models that require that the eigenvalue problem be solved each time the tangent stiffness changes have also been proposed but we decided not to include them since they are computationally expensive and have not been put forth with compelling theoretical support.

Rayleigh Damping with Tangent Stiffness

A generalization of the widely used Rayleigh damping model, introduced to realize a loss of effectiveness during plasticity takes the damping matrix, C, as

$$C = \alpha M + \beta K_T \tag{11}$$

where M = mass matrix, K_T = tangent stiffness matrix and $\alpha, \beta$are constants. The complexity with which the tangent stiffness is formed can vary from the simple elasto-plastic hinges to the much more computationally intensive distributed plasticity models that are widely used in research but less so in conventional seismic engineering practice. Since the model of Eq.11 is the same as the standard Rayleigh model during elastic response, computation of the constants $\alpha, \beta$is not affected by the anticipated nonlinearity. The model in Eq.11 has been around for a long time and is sometimes viewed with reservation because of the abrupt changes in the damping that accompany the changes in stiffness in lumped plasticity models and because it can reach

conditions where the damping can add energy to the system because some eigenvalues turn negative. The first item leads to unbalances that are highly localized in time and have little effect in the global response and the second, except perhaps in studies where the focus is dynamic instability, is seldom active. We take the opportunity to note, however, that a potentially important issue in modeling damping, albeit not restricted to the Rayleigh model, is the appearance of unbalanced forces at massless coordinates [9,10].

Luco and Lanzi (2017)

Luco and Lanzi [6] introduced a model where the damping matrix is taken as

$$C = C_0 K^{-1} K_T \tag{12}$$

where C_0 is any arbitrary damping matrix and K is the initial stiffness. One issue that is worth noting in the model of Eq.12 is that the matrix C is not necessarily symmetrical.

Lanzi and Luco (2018)

Shortly after the appearance of the model in Eq.12 the same authors propose a model for the damping that writes [10]

$$C = K_T K^{-1} C_0 K^{-1} K_T \tag{13}$$

which removes the noted lack of symmetry and eliminates the possibility of negative eigenvalues. The reason for the last observation being that the damping matrix in Eq.13 is a congruent transformation of C_0, and congruent transformations do not change the number of positive, negative and zero eigenvalues of a matrix. A curious byproduct of the same property is the fact that as an eigenvalue of the tangent stiffness approaches zero the dissipation in a particular velocity pattern does the same but if the inelasticity continues and some eigenvalue of the second order tangent stiffness is rendered negative the dissipation increases again.

CSMIPκ

A feature common to all the previous models is that they cannot be modified in the plastic range without changing behavior when the response is linear. The model introduced in this project, which takes the damping matrix as

$$C = \left(\frac{\|K_T\|}{\|K\|}\right)^{\kappa} C_0 \tag{14}$$

where C_0 is arbitrary, $\kappa$is a free parameter and $\|.\|$stands for the 2-norm, has this tunning ability. As can be seen, when $\kappa = 0$ the model reverts to a constant damping matrix and as κincreases the magnitude of the inherent damping during the inelastic response decreases.

On the Damping Matrix for Small Amplitude Response

Evaluation of the *rhs* of Eq.9 requires that a damping matrix for the initial elastic response, C_0 be established; some possibilities are discussed next.

Classical Damping

Any classical damping matrix can be written as

$$C = M\left(\sum_{j=1}^{n} \vartheta_j \phi_j \phi_j^T\right) M \tag{15}$$

where $\vartheta_j = 2\omega_j \xi_j$and ϕ_j, ω_j and $\xi_j$are the mass normalized mode shape, frequency and the damping ratio of the j^{th} mode, respectively. In an experimental setting the rank of the matrix in Eq.15 will equal the number of identified modes and there is, of course, the issue of having only a limited number of monitored levels, which requires that the mode shapes be expanded. The rank issue is not expected to have practical relevance but the need for a significant identification effort followed by modal expansion does not make Eq.15 attractive.

Identification Free Extraction

If the response is measured at all coordinates the damping matrix can be extracted from the data without requiring system identification. The scheme shares with Eq.15 the fact that the mass matrix must be known but no modal truncation is incurred. To illustrate let the seismic response prior to the development of inelastic action be gathered in matrices $\ddot{Y}, \dot{U}, U \in \Re^{n \times N}$containing, as columns, vectors of absolute acceleration, relative velocities and relative displacements, with n=number of levels in the building and N =the total number of time steps used. Since we've assumed that the response is linear during the data collection one can write

$$M\ddot{Y} + C\dot{U} + KU = 0 \tag{16}$$

Selecting $N > n$ guarantees there are right null spaces and taking

$$U\Gamma = 0 \tag{17}$$

one has (from Eq.16)

$$C\dot{U}\Gamma = -M\ddot{Y}\Gamma \tag{18}$$

so the damping matrix is given by

$$C = -M\ddot{Y}\Gamma\left(\dot{U}\Gamma\right)^{+} \tag{19}$$

where the superscript + stands for pseudo inversion. If the mass matrix is known and all the levels are measured Eq.19 would be the method of choice but in the common scenario where only some levels are measured the reconstruction of the response may introduce significant error, so we do not opt for this alternative either.

Mass Proportional Damping

A simple and very convenient approach for our purposes is to take the initial damping matrix as mass proportional. The reason being that in this case both the first and the second terms on the *rhs* of Eq.9 are proportional to M and this eliminates dependence on the actual values of the mass, leaving only the much simpler demand of estimating the relative values. Another attractive feature being that sensor density has no effect on the estimation of C_0 and that all that is required from system identification is an estimate of the frequency and damping of the fundamental mode. There is, in fact, not even a need to separate these two quantities since their product is the real part of the pole of the fundamental mode, which is what is actually computed in the identification. It is true, of course, that the mass proportional model allows control over one mode only, but one suspects that this is not a significant issue in this case.

Response Reconstruction

The large majority of instrumented structures for which records are available have sensors in a subset of all the floors so to apply IDNB it is necessary to reconstruct the response in some levels. Much has been done in this area and there are techniques with various levels of refinement [11,12]. Interpolation schemes are projections of the measurements on a basis that covers the full building height. These bases can be defined using estimated mode shapes or determined by functions that depend on the position of the sensors, as is the case in the widely used Cubic Spline (CS) or can be interpolations of the left side singular vectors of the data matrix (in which case the response can be segmented, and different basis formulated for different time intervals). In all cases, however, if inelasticity produces localized distortions, the results can degrade notably. Consider, for example, a two-story structure where the second floor and the ground are measured, and one is interested in estimating the drift in both levels. In the linear case reasonable results are expected but in the nonlinear case the true response (but not the prediction) will be strongly dependent on the distribution of the inelasticity.

To illustrate quantitatively consider an 8-story shear structure with sensors only on the even number floors and assume one is to reconstruct the unmeasured floors using a cubic spline.

Fig.1 plots the reconstructed absolute acceleration in the 7th level and compares it with the exact result for two conditions, one where the earthquake is scaled so that the response is linear and the other where inelasticity is significant. As can be seen, the accuracy in the case of the linear response is good but in the case with nonlinearity the error is important.

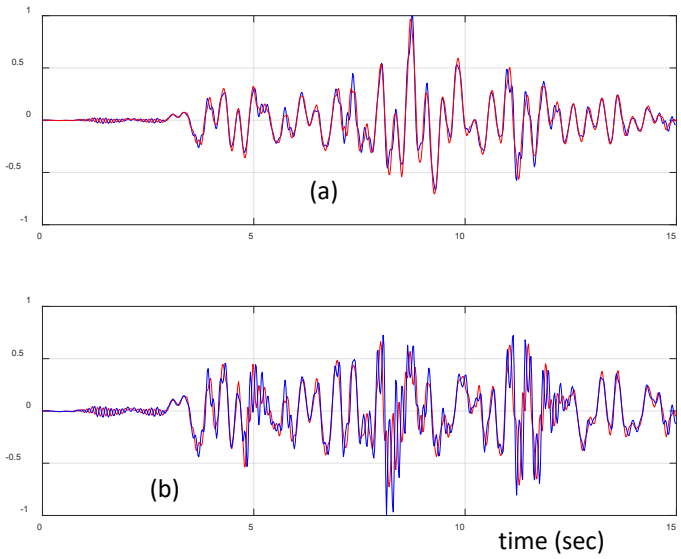

Figure 1. Normalized acceleration on the 7th level of an 8-story structure; reconstructed (in red) and exact result (in blue) for two conditions a) linear response and b) nonlinear response (max story ductility around 3)

Summary of IDNB

- Use a part of the data where (quasi) linear response can be anticipated and some system identification approach to estimate the frequency and damping of the first mode (real part of the first pole) (see *Technical Note*)
- Define the mass proportional damping matrix for small response amplitudes using the above results.
- Select an interpolation scheme and reconstruct the response at unmeasured levels.
- Use the pattern of story weights (actual values not needed) to compute an estimate for the history of the inertial base shear, $V_I(t)$
- Use the mass proportional damping matrix to compute the derivative of the constant damping base shear $\dot{V}_D(t)$ as $r^T C_o \ddot{u}$, where $\ddot{u}$are the relative accelerations
- Differentiate $V_I(t)$numerically.
- Compute $\dot{V}_R(t) = \dot{V}_I(t) + \bar{\rho}\dot{V}_D(t)$for values of $\bar{\rho}$covering some selected range, e.g., $-0.1 \leq \bar{\rho} \leq 1.5$
- Sort $\left|\dot{V}_R(t)\right|$in ascending and decide on $\tilde{t}$.

- Plot the norm of the signal of the previous bullet vs $\bar{\rho}$ and identify the minimum. If the minimum occurs at values of $\bar{\rho}$ that are notably larger than 1 the constraint of Eq.10 is not satisfied and the information on inherent damping during nonlinearity cannot be extracted using IDNB.

Technical Note: Although the response before the strong motion has the damping of the reference state, this segment is just a few seconds long and thus too short to perform a reliable identification. One can use the segment that follows the strong motion, which is typically much longer but must then keep in mind that in this case the $\bar{\rho}$ from IDNB refers to a scaling of the damping that prevails after the strong motion. Although the "late response" linear damping is the same as the one at the outset in common nonlinear models, this is unlikely to be the case in real buildings, especially in the case of concrete. What we've done on this account when IDNB is applied is to take the reference damping as that obtained using the shortest signal (starting at t = 0) for which the first pole appears in the identification, provided this signal does not have a significant fraction in the strong motion region. When the signal that starts at the origin proves too long, we compute the reference damping using the linear response that follows the strong motion.

Validation

To get a sense of what is the best attainable performance we consider the situation where accelerations are available at every level and the damping matrix for small amplitude response is known. For conciseness we limit the examination to an 8-story shear building with a symmetrical plan and consider two ground motions, both recorded during the Northridge earthquake. The masses, story stiffness, and the yield levels are: m=14(1,1,1,1,1,1,1,1}, k=1.91e4{1,1,1,0.7,0.7,0.7,0.5,0.5} and V_y =800{1,1,1,0.9,0.9,0.7,0.7} in units of kips, ft and secs, with the periods of the first 3 modes = {1.0, 0.368,0.232} secs. The simulations are carried out for 4 alternative inherent damping models, namely: a) Constant b) CSMIPκ ($\kappa = 4$) c) Lanzi and Luco and d) Rayleigh with tangent stiffness. The goal is to determine if application of the scheme allows correct identification of models with hysteretic coupling and constant damping.

Ground Motion #1

Ground motion #1 is the record from channel #3 of CSMIP station 24436 during the 17 June 1994, Northridge Earthquake, a station that is located at the Tarzana Cedar Hill Nursery. The record itself, and the shear force vs drift relation for the first story of the model, computed under the premise that the damping is 5% in every mode and uncoupled from hysteresis, are depicted in Fig.2.

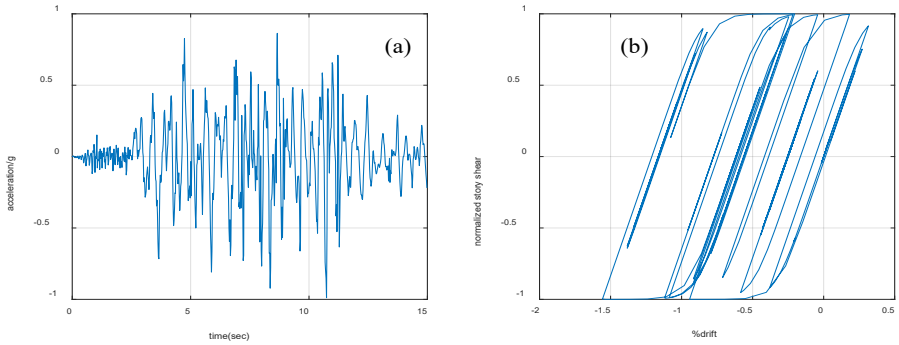

Figure 2. a) ground motion #1 b) first floor shear force drift response.

As can be seen, the inelasticity is significant, with a displacement ductility in the first level slightly larger than 3. The shear force vs drift relationship, as shown in (b), follows a Bouc-Wen model. Fig 3 shows the results from application of IDNB.

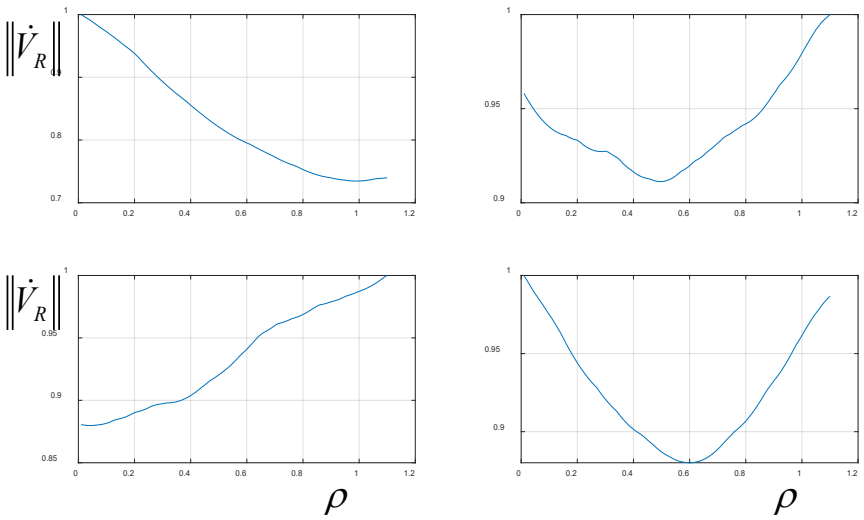

Figure 3. $\|\dot{V}_R\|$ (normalized) for $\tilde{t} = 1.5sec$ ($\Delta t = 0.02sec$) vs $\rho$for a) constant damping b) $CSMIP\kappa$ with $\kappa = 4$ c) Lanzi and Luco d) Rayleigh damping with tangent stiffness (5% in every mode).

As can be seen, the minimum in Fig.3a is reached in the vicinity of 1, correctly pointing to the fact that in this instance the damping matrix is constant. The results in (b) depicts a minimum at around 0.5, which gives an idea of how a nonlinearity with the extent shown in Fig.2 is mapped to $\bar{\rho}$ by the CSMIPκ model with κ =4. For the damping model proposed by Lanzi and Luco the minimum takes place very near zero, suggesting that this model produces large reductions in the inherent damping during the nonlinearity and finally in (d) which shows the result for the Rayleigh model with tangent stiffness, the minimum is only slightly to the left of the result for $CSMIP\kappa$ wit $\kappa = 4$. suggesting that these two models, at least in this example, produce comparable reductions.

Ground Motion #2

We consider the same recording station but use the horizontal record orthogonal to the previous one, which now corresponds to channel 1. The plot of the motion and the shear vs drift relation, which are depicted in Fig.4, show that the extent of inelasticity is somewhat larger than for motion #1. The maximum response ductility reaching a value slightly over 4.

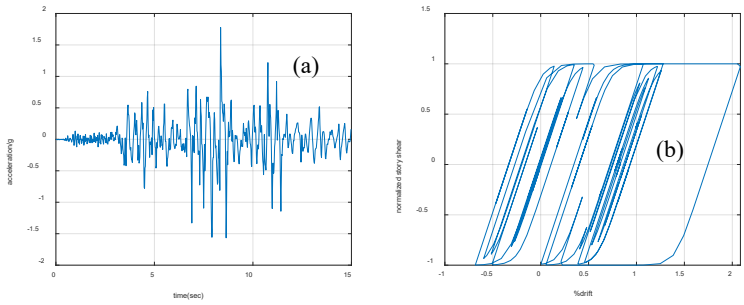

Figure 4. a) ground motion #2 b) first floor shear force drift response.

Instead of repeating the same cases as in Fig.3, we examine results obtained for data generated using the $CSMIP\kappa$ model with different values of κ, namely: 0,2,4 and 6. For$\kappa = 0$the damping is constant and for the others the location of $\bar{\rho}$is expected to shift progressively to the left. The results in Fig.5 confirm these expectations.

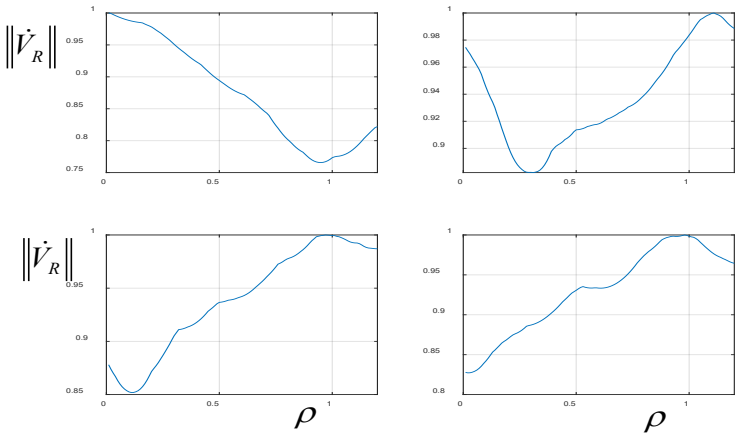

Figure 5. Normalized $\|\dot{V}_R\|$for $\bar{t} = 1.5sec$vs , responses from$CSMIP\kappa$ a-d) $\kappa = 0,2,4,6$, respectively.

IDNB on Real Building Data

CSMIP station 12299

The sensor deployment is depicted in Fig.6. The largest structural response at this station, 0.62g, is for the Palm Spring earthquake of 1986 and we thus choose this record for examination. We select channels {13,12,11,10} in the N-S direction for examination. From inspection of the time history of the excitation the strong is taken to span from time step 100 to 550. System identification showed that (the negative) of the real part of the 1st pole is 0.29. The sampling frequency is 50 Hz.

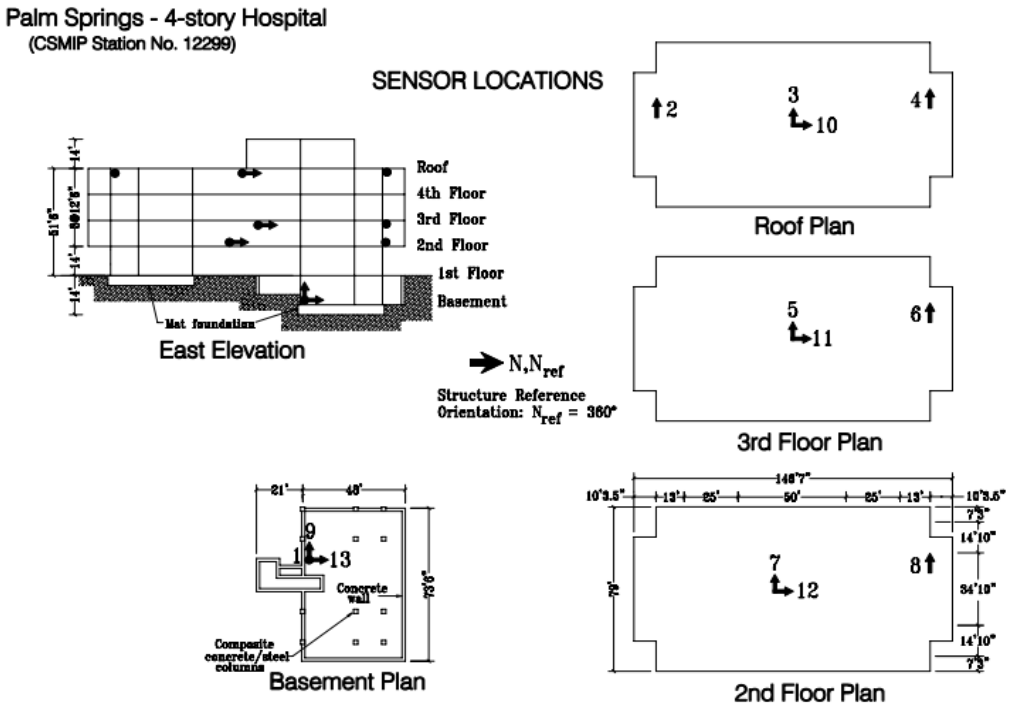

Figure 6. Sensor layout at station 12299

The *rhs* of Eq.7 (normalized) are depicted in Fig.7. The results, as can be seen, are reasonably consistent and point to a reduction in the effectiveness of inherent damping on the order of 50%

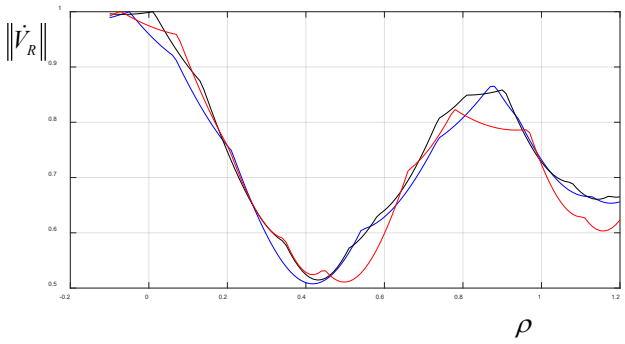

Figure 7. Normalized $\|\dot{V}_R\|$ for $\tilde{t}$=7,8 and 9 Δt.

CSMIP Station 14606

The sensor deployment is depicted in Fig.8. The largest structural response at this station, 0.49g, is for the Northridge earthquake and we chose the response of channels [3,5,8,11] for examination. From inspection of the time history of the input we take the strong motion to span from time step 1200 to 3189. System identification shows that (the negative) of the real part of the 1st pole is 0.447. The sampling frequency is 100 Hz.

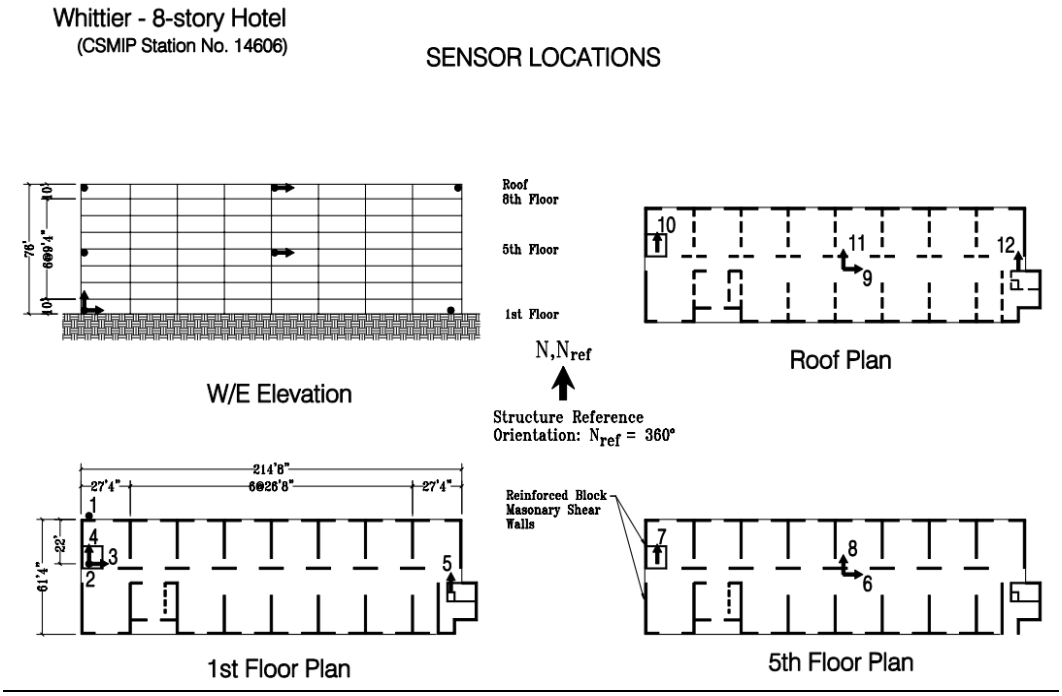

Figure 8. Sensor layout at station 14606

The *rhs* of Eq.7 (normalized) is depicted in Fig.9 for three assumed "yielding" durations. The result, again, is reasonably consistent and point to a reduction in the effectiveness of inherent damping on the order of 60%

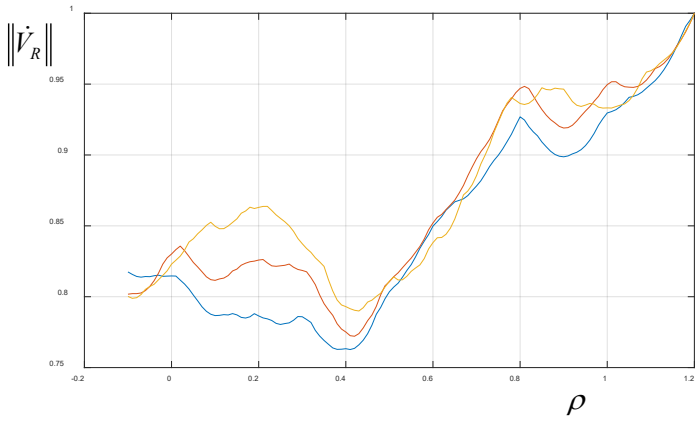

Figure 9. Normalized $\|\dot{V}_R\|$ for $\tilde{t}$=40, 45 and 50 Δt

CSMIP station 24322

The sensor deployment is depicted in Fig.10. The largest structural response at this station, 0.90g, is for the Northridge earthquake and we chose the response to this input for examination. We select the N-S direction and take the input motion (given the rigid basement) as the measurement at the ground floor. The channels used are {11,8,5,2} and we take the strong motion from time step 80 to 570. System identification gives (the negative) of the real part of the 1st pole as 0.091. The sampling frequency is 50 Hz.

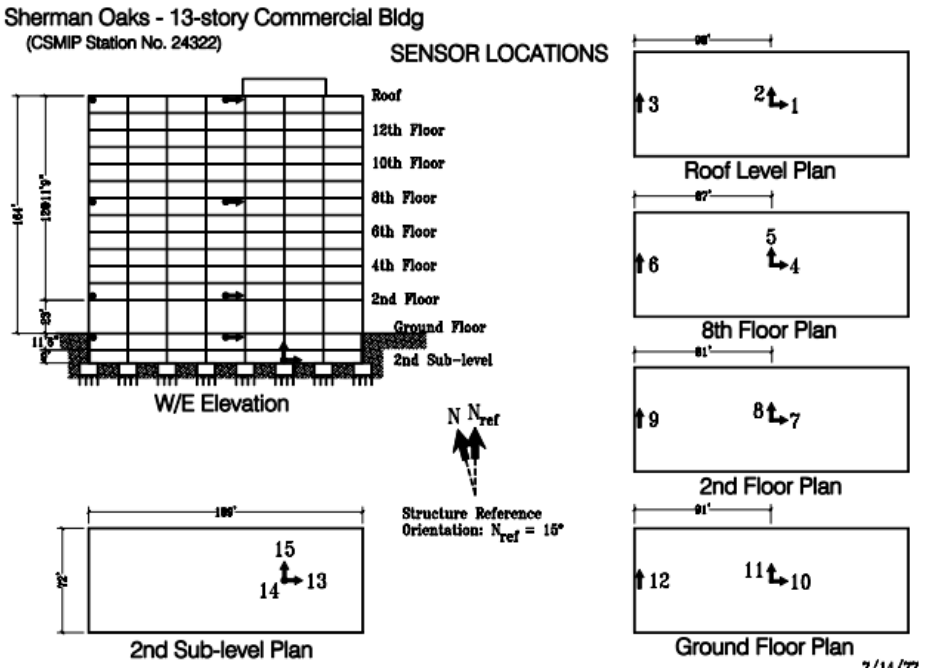

Figure 10. Sensor layout at station 24322.

In this case the results for the scaling constant, as shown in Fig.11, consistently point to a minimum that is reached at a scaling larger than one, indicating (or presumably indicating) that the constraint of Eq.10 is not satisfied. In this case the IDNB interrogation does not hold.

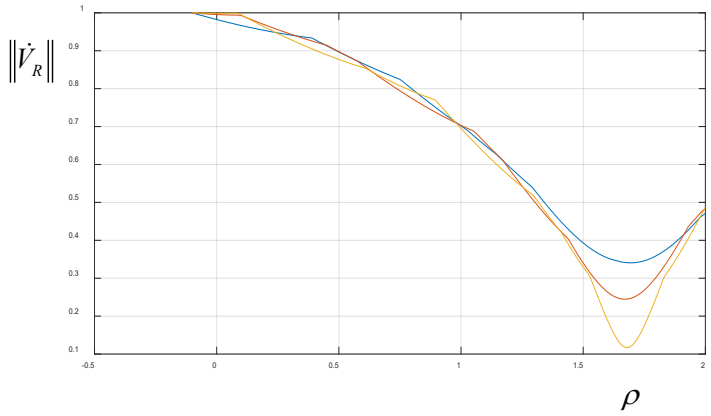

Figure 11. Normalized $\|\dot{V}_R\|$ for $\tilde{t}$=6,8 and 10 Δt.

Concluding Observations

The IDNB scheme attempts to extract information on the behavior of inherent damping during nonlinear excursions by assuming that the rate of change of the base shear during some of these excursions is small enough to be discarded in equilibrium considerations. Since the foregoing assumption is not guaranteed satisfied the approach does not hold for all nonlinear data sets but this is not an important impediment since the goal is not to make assertions about particular structures, but to test which of the two propositions: a) constant pseudo-viscosity or b) some coupling with hysteresis, is the more plausible one. The results thus far suggest that the effectiveness of the inherent damping model may in fact decrease when hysteresis sets in, but it's important to stress that the reliability of this observation is conditional on the validation of IDNB which, at this point, has only been done for responses from shear building models with Bouc-When hysteresis without hardening. Work to determine the reliability of the scheme when the response signals come from more complex nonlinear models is currently ongoing.

References

[1]. Chopra, Anil K., and Frank McKenna. "Modeling viscous damping in nonlinear response history analysis of buildings for earthquake excitation." Earthquake Engineering & Structural Dynamics 45.2 (2016): 193-211.

[2]. Priestley, M. J. N., and D. N. Grant. "Viscous damping in seismic design and analysis." Journal of earthquake engineering 9.spec02 (2005): 229-255.

[3]. Jehel, Pierre, Pierre Léger, and Adnan Ibrahimbegovic. "Initial versus tangent stiffness-based Rayleigh damping in inelastic time history seismic analyses." Earthquake Engineering & Structural Dynamics 43.3 (2014): 467-484.

[4]. Smyrou, Eleni, M. J. Priestley, and Athol J. Carr. "Modelling of elastic damping in nonlinear time-history analyses of cantilever RC walls." Bulletin of Earthquake Engineering 9.5 (2011): 1559-1578.

[5]. Hall, John F. "Problems encountered from the use (or misuse) of Rayleigh damping." Earthquake engineering & structural dynamics 35.5 (2006): 525-545.

[6]. Luco, J. Enrique, and Armando Lanzi. "A new inherent damping model for inelastic time-history analyses." Earthquake Engineering & Structural Dynamics 46.12 (2017): 1919-1939.

[7]. Salehi, Mohammad, and Petros Sideris. "Enhanced Rayleigh damping model for dynamic analysis of inelastic structures." Journal of Structural Engineering 146.10 (2020): 04020216.

[8]. Caughey, T. K. (1960a). “Classical normal modes in damped linear dynamic systems.” J. Appl. Mech., 27(2), 269–271.

[9]. Bernal, Dionisio. "Viscous damping in inelastic structural response." Journal of Structural Engineering 120.4 (1994): 1240-1254.

[10]. Lanzi, Armando, and J. Enrique Luco. "Elastic velocity damping model for inelastic structures." Journal of Structural Engineering 144.6 (2018): 04018065.

[11]. Bernal D., and A. Nasseri. “An approach for response reconstruction in seismic applications”, Proceedings of the 3rd International Operational Modal Analysis Conference IOMAC09, Ancona Italy May 4-6 2009.

[12]. Bernal, D., and A. Nasseri. "Schemes for reconstructing the seismic response of instrumented buildings." SMIP09 Seminar on Utilization of Strong-Motion Data. 2009.